



**HAL**  
open science

## Hybrid plasmonic nanosystem with controlled position of nanoemitters

Aurélie Broussier, Ali Issa, Loïc O Le Cunff, Tien Hoa Nguyen, Xuan Quyen Dinh, Sylvain Blaize, Jerome Plain, Safi Jradi, Christophe Couteau, Renaud Bachelot

► **To cite this version:**

Aurélie Broussier, Ali Issa, Loïc O Le Cunff, Tien Hoa Nguyen, Xuan Quyen Dinh, et al.. Hybrid plasmonic nanosystem with controlled position of nanoemitters. *Applied Physics Letters*, 2019, 114 (16), pp.163106. 10.1063/1.5093360 . hal-03528504v2

**HAL Id: hal-03528504**

**<https://hal.science/hal-03528504v2>**

Submitted on 17 Jan 2022

**HAL** is a multi-disciplinary open access archive for the deposit and dissemination of scientific research documents, whether they are published or not. The documents may come from teaching and research institutions in France or abroad, or from public or private research centers.

L'archive ouverte pluridisciplinaire **HAL**, est destinée au dépôt et à la diffusion de documents scientifiques de niveau recherche, publiés ou non, émanant des établissements d'enseignement et de recherche français ou étrangers, des laboratoires publics ou privés.

# Hybrid plasmonic nanosystem with controlled position of nanoemitters

Cite as: Appl. Phys. Lett. **114**, 163106 (2019); <https://doi.org/10.1063/1.5093360>  
 Submitted: 20 February 2019 • Accepted: 10 April 2019 • Published Online: 26 April 2019

Aurélie Broussier,  Ali Issa, Loïc O. Le Cunff, et al.



View Online



Export Citation



CrossMark

## ARTICLES YOU MAY BE INTERESTED IN

[Photonic thermal conduction by infrared plasmonic resonators in semiconductor nanowires](#)  
 Applied Physics Letters **114**, 163104 (2019); <https://doi.org/10.1063/1.5093309>

[Indium silicon oxide thin films for infrared metaphotonics](#)  
 Applied Physics Letters **114**, 161105 (2019); <https://doi.org/10.1063/1.5089499>

[Midinfrared real-time polarization imaging with all-dielectric metasurfaces](#)  
 Applied Physics Letters **114**, 161904 (2019); <https://doi.org/10.1063/1.5091475>

 QBLOX



1 qubit

Shorten Setup Time

**Auto-Calibration**  
**More Qubits**

Fully-integrated  
**Quantum Control Stacks**  
**Ultrastable DC to 18.5 GHz**  
 Synchronized <<1 ns  
 Ultralow noise



100s qubits

[visit our website >](#)

# Hybrid plasmonic nanosystem with controlled position of nanoemitters

Cite as: Appl. Phys. Lett. **114**, 163106 (2019); doi: [10.1063/1.5093360](https://doi.org/10.1063/1.5093360)

Submitted: 20 February 2019 · Accepted: 10 April 2019 ·

Published Online: 26 April 2019



View Online



Export Citation



CrossMark

Aurélien Broussier,<sup>1</sup> Ali Issa,<sup>1</sup> Loïc O. Le Cunff,<sup>1</sup> Tien Hoa Nguyen,<sup>2</sup> Xuan Quyen Dinh,<sup>2,3</sup> Sylvain Blaize,<sup>1</sup> Jérôme Plain,<sup>1</sup> Safi Jradi,<sup>1</sup> Christophe Couteau,<sup>1</sup> and Renaud Bachelot<sup>1,4,a)</sup>

## AFFILIATIONS

<sup>1</sup>Charles Delaunay Institut (ICD), CNRS, Light, Nanomaterials, Nanotechnologies (L2n) Laboratory, University of Technology of Troyes, 12 rue Marie Curie, 10004 Troyes Cedex, France

<sup>2</sup>CNRS-International-NTU-Thales Research Alliance (CINTRA), 50 Nanyang Drive, Singapore, Singapore 637553

<sup>3</sup>Thales Solutions Asia Pte. Ltd., R&T Department, 21 Changi North Rise, Singapore 498788

<sup>4</sup>Sino-European School of Technology, Shanghai University, 200444 Shanghai, China

<sup>a)</sup>Author to whom correspondence should be addressed: [renaud.bachelot@utt.fr](mailto:renaud.bachelot@utt.fr).

## ABSTRACT

Quantum dots optically excited in close proximity to a silver nanowire can launch surface plasmons. The challenge related to this promising hybrid system is to control the position of nanoemitters on the nanowire. We report on the use of a two-photon photopolymerization process to strategically position quantum dots on nanowires at controlled sites. A parametric study of the distance between the quantum dots and the nanowire extremity shows that precise control of the position of the launching sites enables command of light intensity at the wire end through surface plasmon propagation.

© 2019 Author(s). All article content, except where otherwise noted, is licensed under a Creative Commons Attribution (CC BY) license (<http://creativecommons.org/licenses/by/4.0/>). <https://doi.org/10.1063/1.5093360>

Nanoplasmonics is an area of increasing interest. One of the most recent and promising research topics is hybrid nanoplasmonics that attempts to control the energy transfer between nanoemitters and surface plasmons (SPs).<sup>1,2</sup> SPs are collective electronic coherent oscillations coupled to electromagnetic surface waves that are evanescently confined at the interface between a metal and a dielectric medium. Silver nanowires (Ag-NWs) are metal nanostructures which support propagative SPs that can be launched or detected at the nanowire's extremities.<sup>3,4</sup> Semiconductor nanocrystals, better known as quantum dots (QDs), are good nanoemitters<sup>5</sup> due to their unique set of optical properties, which occur from a quantum confinement effect.<sup>6</sup> Their optical properties make them suitable candidates for light emitting hybrid plasmonic nanosystems.<sup>7</sup> In particular, they allow working at specific emission wavelengths through their size and composition.<sup>8</sup> The position of the QDs, however, has to be accurately controlled relative to the metal nanostructure in order to obtain efficient and reliable nanoemitter-metal nanostructure coupling and energy transfer.

Over the past decade, energy transfer between QDs and plasmonic structures (including metal NWs) has been giving rise to many reported studies (e.g., Refs. 9–11). Most of them used spin coating as a deposition technique of QDs onto the plasmonic system.<sup>11–13</sup> Spin

coating is a quick and simple solution, but does not permit any control of the position of the QDs relative to the metal nanostructure. As a result, many samples must be made before obtaining a satisfactory one where the QD location is suitable for physical studies of interest. Some other reported studies still used spin coating to deposit the QDs, but then used either electron beam lithography<sup>14</sup> or atomic force microscopy<sup>15</sup> to place the nanoparticles at strategic locations. Other articles reported on the use of a layer of polyethylene, which captures QDs that are in aqueous solution,<sup>16,17</sup> while others use a ligand molecule to graft QDs onto metallic nanoparticles.<sup>18–20</sup> Similarly, QD functionalization can also be used to have QDs on plasmonic structures.<sup>21</sup> Finally, photopolymerization around metallic nanoparticles through the excitation of localized SPs, and involving evanescent waves turned out to be an efficient solution to strategically place QDs around them.<sup>22</sup> Following on from this local photopolymerization idea, we propose an even simpler and faster solution for more precisely positioning QDs on plasmonic structures that support the propagating surface plasmons. Our approach of nanoemitter positioning is based on the far-field two-photon polymerization (2-PP) of QD-containing photosensitive materials that was used and described in Refs. 22 and 23. In Ref. 22, using such a hybrid photosensitive material, we

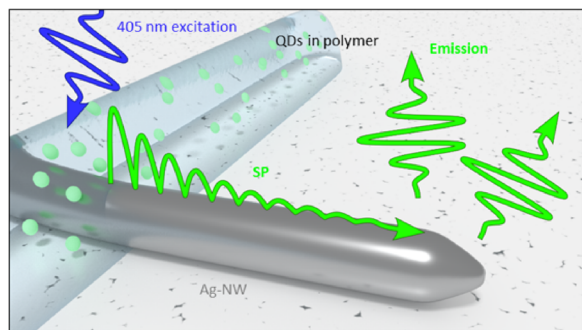


**FIG. 1.** Representation of the developed hybrid nanosystem based on coupling between light emitting quantum dots (QDs) in polymer and surface plasmons (SPs) supported by a silver nanowire (Ag-NW).

demonstrated local trapping of QDs around metal nanostructures. Based on metal nanostructure evanescent plasmonic near-fields to trigger 2-PP, polarization sensitive hybrid nanoemitters were the result. In this letter, we report on a controlled hybrid plasmonic nanoemitter (see the illustration in Fig. 1) based on coupling between CdSe/ZnS QDs and propagating SPs that are supported by silver nanowires (Ag-NWs considered as SP resonators<sup>24</sup>) and observed though their scattering at the nanowire ends.<sup>11,25</sup>

While QDs/Ag-NW coupling has already been reported (e.g., Ref. 26), it is emphasized that we place the QDs at different distances from the Ag-NW extremity by 2-PP with a spatial precision that allows for well-defined plasmon launching sites and scattered photoluminescence (PL) intensity at the NW extremity, as well as quantitative determination of the SP propagation length (see the illustration in Fig. 1).

The Ag-NWs (Sigma-Aldrich, ref. 739448) were diluted in an isopropanol solution and have a length dispersion ranging from 5 to 50  $\mu\text{m}$ . Samples were prepared by spin coating a solution of silver nanowires in isopropanol onto a clean glass substrate at 3000 r.p.m for 30 s. Scanning Electron Microscopy (SEM) showed that the average nanowire has a diameter in the 130–160 nm range and is of monocrystalline in nature.<sup>27</sup> Chemically grown monocrystalline Ag-NWs are characterized by smooth defect-free surfaces and faceted ends, as shown in the SEM images in Fig. 2(a).

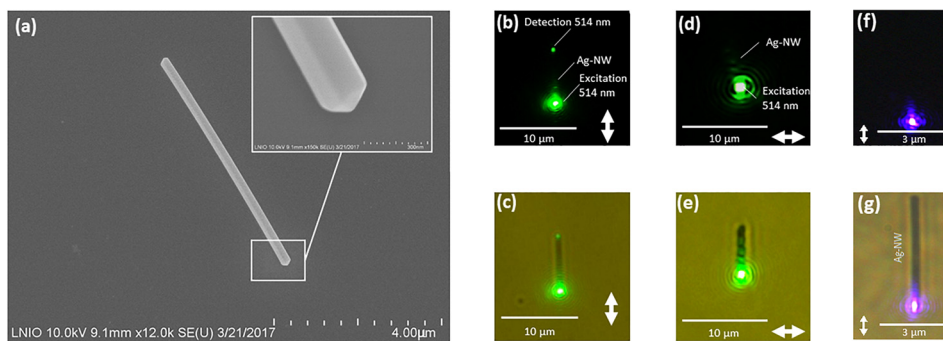


**FIG. 2.** (a) SEM image of an Ag-NW on a Si substrate. Inset: Zoom-in view at the NW extremity. (b) A 7  $\mu\text{m}$  long Ag-NW illuminated by a focused green beam polarized along the wire axis, (c) Same as (b) with white light. (d) The same Ag-NW as (a) illuminated by a focused green beam polarized perpendicular to the wire axis. (e) Same as (d) with white light. (f) A 5  $\mu\text{m}$  long Ag-NW illuminated by a focused laser at a 405 nm beam polarized parallel to the wire axis. (g) Same as (f) with white light. The white arrows represent the incident polarization direction.

By focusing the laser light ( $\lambda = 514 \text{ nm}$ ) onto the Ag-NW end, SPs are excited and launched, as evidenced by the green light emission spot at the other end, resulting from SP perturbation and scattering [Figs. 2(b) and 2(c)]. The nanowire end geometry allows one to couple SPs to propagating waves. No SP excitation was observed when the laser is focused on the NW body, far from its extremities, showing that the sharp NW extremities shown in the inset of Fig. 2(a) enable, through scattering, generation of a large range of high in-plane wave vectors that match the SP dispersion function at this wavelength. The excitation of SP modes using this end-scattering coupling scheme is dependent on the polarization of the incident light.<sup>28</sup> Because of their partly longitudinal nature as a wave, SPs can be excited for an incident polarization parallel to the NW axis [Figs. 2(b) and 2(c)], but not for an incident polarization perpendicular to the axis [Figs. 2(d) and 2(e)], confirming that those Ag-NWs are interesting candidates for supporting SPs propagating along their axis in the green range.

It should be pointed out that no SP propagation was observed in the case of NW excitation at 405 nm wavelength, which is the wavelength used for QD excitation in the following. In Figs. 2(f) and 2(g), a 405 nm wavelength beam was focused onto the NW end with polarization parallel to the NW. Despite the pretty NW short length (5  $\mu\text{m}$ ), no measurable scattered light was obtained at the other extremity. No efficient SP mode can thus be directly excited at this wavelength. Numerical simulations showed that 405 nm excitation can however lead to the excitation of a propagative surface plasmon whose intensity decay length is about 300 nm on a bare Ag-NW, with an effective wavelength of 313 nm. As is shown in Fig. 5, this propagation length can be even shorter in the presence of a sulfur layer on the NW.

Nanoemitters were integrated by local 2-PP of photosensitive formulation made of 1% Irgacure 819 (IRG 819) and 99% QDs-grafted pentaerythritol triacrylate (PETIA).<sup>22,23</sup> CdSe/ZnS QDs with an emission wavelength centered on 510 nm were used. The photopolymerization process was achieved, thanks to a femtosecond laser at  $\lambda = 780 \text{ nm}$  focused by a  $100\times/1.3\text{NA}$  oil immersion objective. This wavelength matches the IRG819 absorption peak at a wavelength of 368 nm. Two-photon absorption within the tight focal point of the laser focused inside the photosensitive formulation leads to polymerization reaction when the exposure energy dose exceeds a given threshold  $D_{th}$  that was precisely assessed by a far-field prestudied before the experiment.<sup>29</sup>

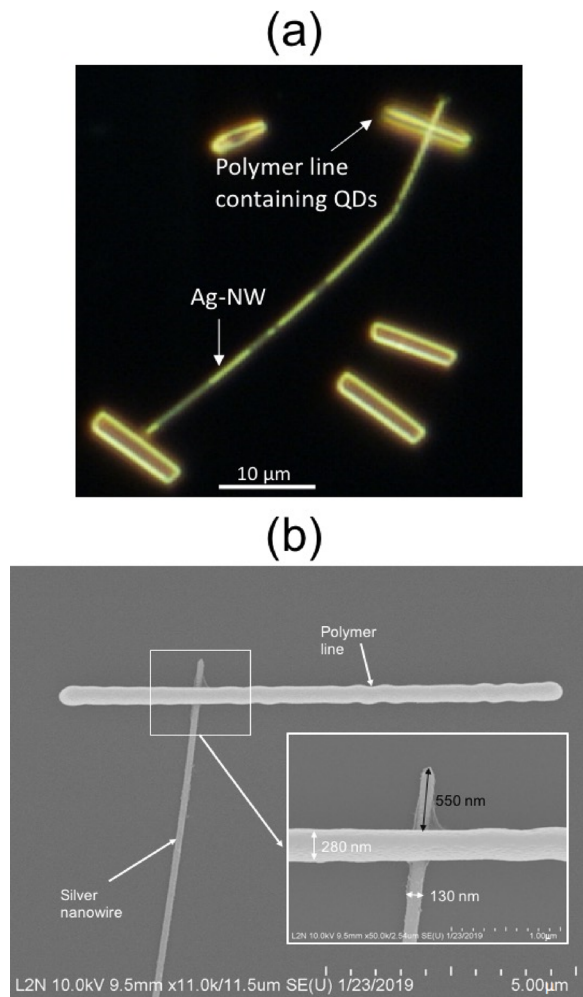


**FIG. 3.** Hybrid plasmonic nanostructures consisting of a Ag-NW coupled with QD-containing polymer lines that were written by 2-PP. (a) Dark-field white light optical image. (b) SEM image. Inset: Zoom-in view at the crossing point between the silver nanowire and the polymer line.

Since QDs were grafted onto the monomers in solution, they can get firmly trapped within the resulting polymer structure. The remaining liquid unpolymerized QD-containing solution was removed by rinsing with acetone for 10 min, followed by HCl for 10 min and isopropanol for 10 min.

Practically, the Ag-NWs were deposited on a glass substrate by spin coating. A drop of photopolymerizable formulation was deposited on the sample. Then, a line of QDs-containing polymer was drawn perpendicularly to the NW axis through 2-PP laser scanning (*Nanoscribe GmbH*) with an incident dose slightly higher than  $D_{th}$  (see the schematic in Fig. 1). Figure 3 shows the typical resulting hybrid systems consisting of a Ag-NW surrounded by written QD-containing polymer lines. In the SEM image, Fig. 3(b), these lines have a typical width in the 250–300 nm range, but 70 nm wide lines could be obtained under specific conditions at  $\lambda = 780$  nm exposure.<sup>23</sup> Several polymer lines were made on several nanowires in order to

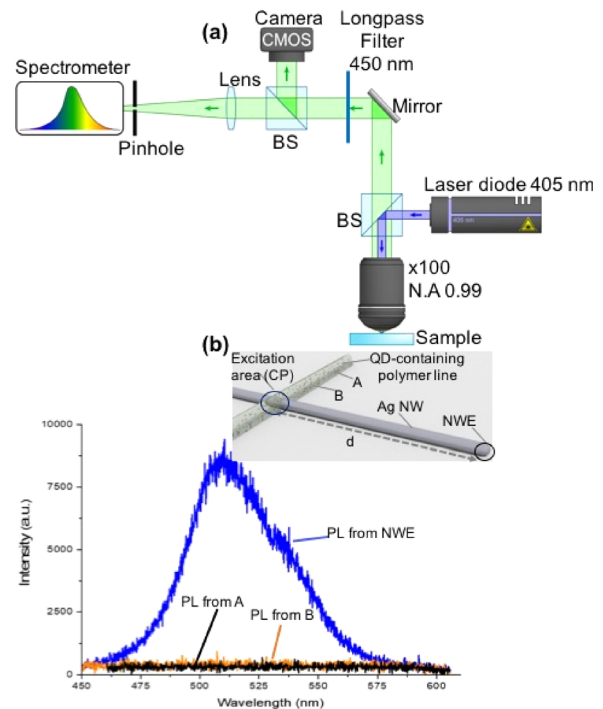


**FIG. 4.** Local photoluminescence (PL) from the hybrid plasmonic nanosystem: (a) Optical set-up. (b) PL spectrum from different areas. Blue curve: from the nanowire extremity (NWE). Black and orange curves: from the polymer line outside the nanowire (A and B locations). The excitation area (CP, 405 nm wavelength) is fixed. The CP-NWE distance  $d$  is a controlled parameter.

carry out a parametric study of the effect of  $d$ , the distance between the QD location and the NW end.

QDs were used to launch SPs on Ag-NWs. The optical set-up consists of a home-made confocal microscope with a 405 nm excitation wavelength from a cw laser [Fig. 4(a)]. The incident laser beam

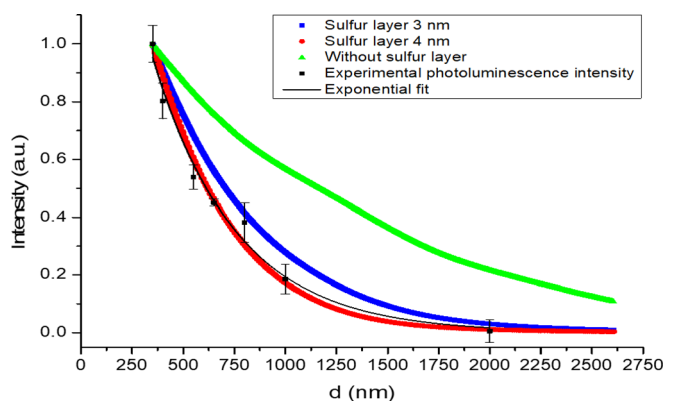


**FIG. 5.** PL Intensity at the nanowire extremity. Black dots: PL intensity measured at the NWE as a function of the distance  $d$  between the NWE and the polymer line. Black curve: exponential fit. Green curve: simulated intensity along a Ag-NW without a sulfurization layer. Blue and red curves: simulated intensity along a Ag-NW with a sulfurization layer (3 nm and 4 nm thickness, respectively).

was focused using a Nikon Plan 100 $\times$  objective of N.A. = 0.99. A long-pass filter at 450 nm allows one to collect only the QD emission. A pin-hole was used to select a specific detection area on the sample in order to collect the local photoluminescence. Both the detection area and the focused laser beam have a diameter of about 250 nm, which is larger than the diameter of the Ag-NW and much smaller than the NW length.

Figure 4(b) shows different local PL spectra taken at different locations, while the 405-nm wavelength excitation area was fixed and localized at the crossing point (CP) between the NW and the QD-containing polymer line. The CP and the NW end (NWE) are separated from each other by a controlled distance  $d$ . Measurable PL spectra centered at 510 nm were obtained only at the NWE [blue spectrum in Fig. 4(b)] and at the CP. In particular, no PL signature was observed when the laser was placed at the polymer line [orange and black spectra in Fig. 4(b)] and at the NW body, between the CP and the NWE. The only possibility for observing an emission at the NWE was to place the excitation laser at the CP.

The fact that PL was observed at the NW end suggests an energy transfer between excited QDs (at the CP) and the NW end *via* SP propagation: QDs were excited in close proximity to a Ag-NW, the QD near-field emission was transferred into guided propagating NW surface plasmons that were scattered at the NW end. While NW surface plasmons were directly excited in the green in Figs. 2(b) and 2(c), green surface plasmons were excited in an inelastic way, *via* QD emission, in Fig. 4(b). It should be reminded that no direct SP excitation is possible with a 405 nm wavelength [see Figs. 2(f) and 2(g)]. In addition, the effective SP wavelength  $\lambda_{SPP}$  was calculated in the case of 514 nm excitation. We found  $\lambda_{SPP} = 450$  nm, which is pretty far from 405 nm, making unlikely excitation of this SP mode with UV light excitation. In conclusion, only QD PL emission can be the cause of SP excitation.

Compared with metallic nanoparticles, the Ag-NW enables the propagation of SPs in a well-defined direction along the NW,<sup>14</sup> making possible long-distance energy transfer between the nanoemitter and a specific NW point of interest. The possibility to place the nanoemitters in a controlled way is a clear asset as is shown in Fig. 5.

The energy transfer between QDs and metallic nanoparticles is governed by dipole-dipole interactions, and the transfer rate between CP and the NWE is determined by both SP excitation efficiency (EE) at the CP and SP propagation decay. At the CP, the orientation and position of QD dipoles are supposed to be random. The EE depends on three main parameters: QD dipole orientations (since surface plasmons are longitudinal waves, mainly dipoles parallel to the NW are expected to excite the plasmon mode), their distance from the NW, and the spectral overlap between the plasmon modes and the QD emission.<sup>24</sup> It is assumed that the EE is constant whatever the position of the CP (i.e., whatever  $d$  is).

A parametric study of plasmon propagation was performed. Several hybrid structures were made to study the influence of  $d$ , the distance between the CP and the NW end [see Fig. 4(b)]. In other words, we controlled, by 2-PP, the position on the metal nanowire of the nanoemitter-containing site that acts as a plasmon launching site.

Figure 5 shows the results of the study. The measured PL intensity detected at the NWE is plotted as a function of  $d$  (black squares). Each point is the mean value of ten successive measurements on the same structure. It should be pointed out that  $d$  is actually the distance

between the NWE and the center of the polymer line whose width is about 280 nm [see Fig. 3(b)]. For each point, PL intensity at the NWE was normalized by the PL intensity directly detected right at the CP. The PL intensity at the NWE exponentially decreases as  $d$  increases, which is the signature of a propagating SP whose intensity can be described as follows:<sup>30</sup>

$$I = I_0 e^{-\alpha x} = I_0 e^{-\frac{d}{L_{SPP}}}, \quad (1)$$

with  $\alpha$  being the attenuation coefficient and  $L_{SPP}$  the plasmon propagation length. It should be pointed out that  $I_0$  depends on at least four parameters: incident exciting intensity, QD absorption rate, quantum yield (QY = 0.6) and excitation efficiency (defined above). The excitation efficiency, the QY and the absorption rate are supposed to be constant, and the measured intensity was normalized by the incident intensity.  $I_0$  is thus considered constant for any  $d$  value.

Figure 5 shows a clear dependence on  $d$ , showing that it is possible to control the PL intensity at the NWE by controlling the position of the launching site.

Due to the SP propagation loss, the emission intensity decays exponentially with respect to the propagation distance as shown by Eq. (1). By fitting the PL intensity using the exponential form (black curve in Fig. 5), the SP propagation length can be quantified. In our study, the SP propagation length for excitation at 510 nm by QDs in polymer was found to be around 407 nm, which is lower than expected. Indeed, the typical SP propagation length on silver can reach a value of 1.1  $\mu\text{m}$  for green light.<sup>31</sup> Spatial decay of Ag-NW SPs launched by a dipole was calculated by the Finite Difference Time Domain (FDTD) method (see supplementary material). The resulting exponential decay shown in Fig. 5 (green curve) confirms a propagation length  $>1 \mu\text{m}$ . This significant difference is interpreted as follows. The SP propagation length can strongly decrease due to either surface roughness or formation of silver sulfide at the Ag-NW surface.<sup>32,33</sup> The effect of surface roughness can be ruled out for chemically synthesized Ag-NWs. However, the HCl used for the rinsing procedure most probably removed the protective layer around the nanowires, making possible sulfurization of NWs. We ran several FDTD simulations with different sulfur layer thicknesses (see supplementary material). Each simulation was designed as follows: an Ag-NW is encased in a thin silver sulfide shell [ $n = 3.1 + 0.65i$  (Ref. 34)] and is placed onto a glass substrate. The sulfurized wire was then excited through a dipole placed close to its surface, which can thus get coupled to SPs. The field intensity along the wire was calculated. In Fig. 5, blue and red curves represent the calculated intensity decay in the presence of 3 nm and 4 nm thick sulfur layers, respectively. The theoretical SP propagation length was accessed in both cases: 3 nm-thick sulfur layer leads to  $L_{SPP} = 510$  nm that drops to about 400 nm for the 4-nm sulfur thickness. SP propagation is thus strongly affected by the presence of this sulfur layer. We can deduce that the Ag-NWs have endured sulfurization and that the sulfur layer is about 4 nm. This result implies that, in case Ag-NWs are used for nanophotonic applications, control of the atmosphere surrounding them is critical. Alternatively, Ag-NWs could be protected by a thin dielectric layer of controlled thickness.

In conclusion, Ag-NW supporting propagating SPs is a fundamental building block of plasmonic integrated circuits. The NW can get coupled with light emitting QDs, providing a promising integrated platform for optical information propagation and processing. Our work shows that it is possible to place QDs on the Ag-NW at

controlled sites, by 2-PP of a designed QD-containing photosensitive formulation. First, we have shown experimentally that the QD emission can excite Ag-NW SPs from a well-defined launching site. The launched SPs propagate along the NW axis. By scattering, light is emitted from the NW extremity. 2-PP allowed one to carry out a parametric study of the distance between the integrated QDs and the Ag-NW end. With this study, we showed that light intensity at the NW extremity can be controlled by controlling the position of the launching site, through the SP propagation length that could be precisely determined.

Its prospective is numerous. In particular, much thinner polymer lines<sup>23</sup> will be used to identify the launcher position in a more precise way and to integrate single QDs by controlling both the line width and the QD concentration within the formulation. In addition, this approach is very promising to produce efficient acceptor-donor hybrid nanosystems by using different kinds of QD-containing photopolymerizable formulations.<sup>22,23</sup>

See [supplementary material](#) for a detailed description of FDTD calculation.

Experiments were carried out within the Nanomat platform ([www.nanomat.eu](http://www.nanomat.eu)). This project was financially supported by the ANR (French Research Agency) and the NRF (National Research Foundation, Singapore) through the International ACTIVE-NANOPHOT (alias "MULHYN") funded project (ANR-15-CE24-0036-01 and NRF2015-NRF-ANR000-MULHYN).

## REFERENCES

- D. Bouchet, E. Lhuillier, S. Ithurria, A. Gulinatti, I. Rech, R. Carminati, Y. De Wilde, and V. Krachmalnicoff, *Phys. Rev. A* **95**, 033828 (2017).
- V. N. Pustovit, A. M. Urbas, and T. V. Shahbazyan, *J. Opt.* **16**, 114015 (2014).
- H. Wei and H. Xu, *Nanophotonics* **1**, 155–169 (2012).
- M. Song, J. Dellinger, O. Demichel, M. Buret, G. Colas Des Francs, D. Zhang, E. Dujardin, and A. Bouhelier, *Opt. Express* **25**, 9138 (2017).
- D. J. Norris and M. G. Bawendi, *Phys. Rev. B* **53**, 16338 (1996).
- H. Haug and S. W. Koch, *Quantum Theory of the Optical and Electronic Properties of Semiconductors*, 5th ed. (World Scientific Publishing Company, 2009).
- J. M. Luther, P. K. Jain, T. Ewers, and A. P. Alivisatos, *Nat. Mater.* **10**, 361 (2011).
- Y. Zhang and A. Clapp, *Sensors* **11**, 11036 (2011).
- M. Pfeiffer, K. Lindfors, C. Wolpert, P. Atkinson, M. Benyoucef, A. Rastelli, O. G. Schmidt, H. Giessen, and M. Lippitz, *Nano Lett.* **10**, 4555 (2010).
- J. Bellessa, C. Bonnard, J. C. Plenet, and J. Mugnier, *Phys. Rev. Lett.* **93**, 036404 (2004).
- Q. Li, H. Wei, and H.-X. Xu, *Chin. Phys. B* **23**, 097302 (2014).
- A. V. Akimov, A. Mukherjee, C. L. Yu, D. E. Chang, A. S. Zibrov, P. R. Hemmer, H. Park, and M. D. Lukin, *Nature* **450**, 402 (2007).
- G. Lamri, A. Movsesyan, E. Figueiras, J. B. Nieder, J. Aubard, P.-M. Adam, C. Couteau, N. Felidj, and A.-L. Baudrion, *Nanoscale* **11**, 258 (2019).
- J.-H. Song, T. Atay, S. Shi, H. Urabe, and A. V. Nurmikko, *Nano Lett.* **5**, 1557 (2005).
- P. Kolchin, N. Pholchai, M. H. Mikkelsen, J. Oh, S. Ota, M. S. Islam, X. Yin, and X. Zhang, *Nano Lett.* **15**, 464 (2015).
- V. K. Komarala, A. L. Bradley, Y. P. Rakovich, S. J. Byrne, Y. K. Gun'ko, and A. L. Rogach, *Appl. Phys. Lett.* **93**, 123102 (2008).
- M. Lunz, V. A. Gerard, Y. K. Gun'ko, V. Lesnyak, N. Gaponik, A. S. Susha, A. L. Rogach, and A. L. Bradley, *Nano Lett.* **11**, 3341 (2011).
- E. Oh, M.-Y. Hong, D. Lee, S.-H. Nam, H. C. Yoon, and H.-S. Kim, *J. Am. Chem. Soc.* **127**, 3270 (2005).
- R. Schreiber, J. Do, E.-M. Roller, T. Zhang, V. J. Schüller, P. C. Nickels, J. Feldmann, and T. Liedl, *Nat. Nanotechnol.* **9**, 74 (2014).
- S. T. Kochuveedu, T. Son, Y. Lee, M. Lee, D. Kim, and D. H. Kim, *Sci. Rep.* **4**, 4735 (2014).
- Y. Lee, S. H. Lee, S. Park, C. Park, K.-S. Lee, J. Kim, and J. Joo, *Synth. Met.* **187**, 130 (2014).
- X. Zhou, J. Wenger, F. N. Viscomi, L. Le Cunff, J. Béal, S. Kochtcheev, X. Yang, G. P. Wiederrecht, G. Colas des Francs, A. S. Bisht, S. Jradi, R. Caputo, H. V. Demir, R. D. Schaller, J. Plain, A. Vial, X. W. Sun, and R. Bachelot, *Nano Lett.* **15**, 7458 (2015).
- Y. Peng, S. Jradi, X. Yang, M. Dupont, F. Hamie, X. Q. Dinh, X. W. Sun, T. Xu, and R. Bachelot, *Adv. Mater. Technol.* **4**, 1800522 (2019).
- H. Ditlbacher, A. Hohenau, D. Wagner, U. Kreibig, M. Rogers, F. Hofer, F. R. Aussenegg, and J. R. Krenn, *Phys. Rev. Lett.* **95**, 257403 (2005).
- Y. Fang, H. Wei, F. Hao, P. Nordlander, and H. Xu, *Nano Lett.* **9**, 2049 (2009).
- H. Wei, D. Ratchford, X. Li, H. Xu, and C.-K. Shih, *Nano Lett.* **9**, 4168 (2009).
- Y. Sun, B. Gates, B. Mayers, and Y. Xia, *Nano Lett.* **2**, 165 (2002).
- Z. Li, K. Bao, Y. Fang, Y. Huang, P. Nordlander, and H. Xu, *Nano Lett.* **10**, 1831 (2010).
- H. Ibn El Ahrach, R. Bachelot, A. Vial, G. Léronde, J. Plain, P. Royer, and O. Soppera, *Phys. Rev. Lett.* **98**, 107402 (2007).
- S. A. Maier, *Plasmonics: Fundamentals and Applications* (Springer Science & Business Media, 2007).
- J. de Torres, P. Ferrand, G. Colas des Francs, and J. Wenger, *ACS Nano* **10**, 3968 (2016).
- J. Zeng, J. Tao, D. Su, Y. Zhu, D. Qin, and Y. Xia, *Nano Lett.* **11**, 3010 (2011).
- M. Rycenga, C. M. Copley, J. Zeng, W. Li, C. H. Moran, Q. Zhang, D. Qin, and Y. Xia, *Chem. Rev.* **111**, 3669 (2011).
- J. M. Bennett, J. L. Stanford, and E. J. Ashley, *J. Opt. Soc. Am.* **60**, 224 (1970).